ENGINEERING DESIGN OF MAN-MADE FIBROUS TEXTILE STRUCTURE TO OPTIMIZE THERMAL COMFORT PROPERTIES

Synopsis of the Ph.D. Thesis

Submitted by

Sujit Shrikrushnarao Gulhane

(Roll No 70821017013)

Department of Textile Engineering

Supervisor

Dr. V. S. Shivankar

submitted in partial fulfilment of the requirements of

DOCTOR OF PHILOSOPHY (Engineering)

MUKESH PATEL SCHOOL OF TECHNOLOGY MANAGEMENT & ENGINEERING
SVKM's NARSEE MONJEE INSTITUTE OF MANAGEMENT STUDIES (Declared as Deemed-to-be University Under Section 3 of the UGC Act, 1956)
V. L. Mehta Road, Vile Parle (West)
MUMBAI –400056

January 2024

TABLE OF CONTENTS

1 ABSTRACT 1

2 INTRODUCTION 2

3 OBJECTIVES 3

4 LITERATURE REVIEW 4

4.1 Developments in Fabric Structure for Enhancing Moisture Management Properties 4

4.2 Finishing Techniques for Improved Moisture Management 7

5 CONTRIBUTION 9

5.1 Wicking Properties of Polyester Filament Yarns Used in Sportswear 9

5.2 Wicking Properties of Polyester Filament Yarn Knitted Fabrics Used in Sportswear 11

5.3 Wicking Performance of C-Shape Filament Yarn for Comfort Fabrics 15

5.4 Fabric Moisture Management Assessment through Advanced Image Analysis 28

6 CONCLUSION 30

7 FUTURE SCOPE 31

7.1 Future Directions for Enhanced Comfort in Man-Made Fibrous Textiles 31

8 PUBLICATIONS 32

9 REFERENCES 33

LIST OF FIGURES

Figure 5.1: Fabric Samples Tested for Wicking 12
Figure 5.2: Microscopic image of the C Shape filament yarn 16
Figure 5.3: Experimental setup for yarn vertical wicking test(Patnaik et al. 2006) ..... **Error! Bookmark not defined.**
Figure 5.4: Pore structure in hexagonally packed yarn (Das et al. 2011). 22
Figure 5.5: a) Packing of filament in Yarn b) Unit area of yarn c) Area occupied by the filament 23
Figure 5.6: Structure of C-shaped filament used for calculating area occupied by the filament.. 24
Figure 5.7: a) Geometrical arrangement of filaments in Yarn dimension b) Unit area of Yarn. .....**Error! Bookmark not defined.**
Figure 5.8: Area occupied by the a) circular filament and b) C Shape filament.**Error! Bookmark not defined.**

LIST OF TABLES

Table 5.1: Wicking test results of the yarn samples. 10
Table 5.2: Vertical Wicking in Wale and Course Direction 13
Table 5.3: Horizontal Wicking Area in mm2 After 1 Minute 14
Table 5.4: The Dimensions of Circular and C-Shaped Filament Yarns 17
Table 5.5: Maximum Wicking Hight of Circular Cross-Section Filament Yarns 17
Table 5.6: Maximum Wicking Hight of C-Shape Cross-Section Filament Yarns 17
Table 5.7. Maximum Wicking Height of Circular Cross-Section Filament Yarns. 26
Table 5.8. Maximum Wicking Height of C-Shape Cross-Section Filament Yarns. 27
Table 5.9. Measured Wicking Area in mm square 29

1 ABSTRACT

The thesis, titled "Engineering Design of Man-Made Fibrous Textile Structure to Optimize Thermal Comfort Properties," is extensively examined, with man-made fibre (MMF), particularly polyester, constituting 60% of the global fibre market share. The surge in MMF usage is contextualized in the introductory section, driven by fitness trends and the fashion industry's reliance on synthetic fibres. Despite the inherent advantages of MMF, the challenges in achieving optimal thermal comfort in MMF textiles are focused on in the thesis. The goal is to contribute to the fundamental understanding of liquid moisture management in MMF textiles and provide practical solutions to enhance their thermal comfort properties.

Strategies, including blending hydrophilic fibres, are explored in the literature review to counter the innate hydrophobic nature of synthetic fibres. Physical finishing processes, like calendaring and plasma treatment, are examined for their role in enhancing moisture absorption and wicking by modifying fabric structure. Despite potential long-term efficacy concerns, promising avenues emerge with chemical finishing methods, such as cationization and hydrophilic polymer application. The importance of physical modifications in fabric structure for sustainable and enduring enhancements in moisture management for synthetic fabrics is underscored in the chapter.

The investigation into polyester filament yarns provides insights into filament denier, cross-sectional shape, and intermingling processes, offering valuable optimization strategies for sportswear performance. The study extends to knitted fabrics, emphasizing the pivotal role of fabric structure in water absorption for sportswear applications. Superior wicking performance is exhibited by C-shaped cross-section filament yarns, making them a good choice for comfortable fabrics in sportswear and activewear. The optimization of filament yarn design and enhancement of wicking performance is integrated through theoretical models and experimental validation.

The thesis concludes by introducing the Moisture Management Tester, a novel tool for fabric moisture assessment. Its efficiency, automation, and time-dependent analysis make it a valuable asset for research and production in the textile industry.

2 INTRODUCTION

In the dynamic landscape of global textile consumption, Man-Made Fibre (MMF) emerged as the cornerstone, constituting a substantial 60% of the overall fibre market share, with polyester fibre taking the forefront. The global demand for fibres experiences a notable surge, escalating from 87 million tons in 2014 to a staggering 103 million tons in 2022, and polyester assumes the mantle as the largest and fastest-growing category, boasting a current global consumption of 57 million tons. This transformative shift towards MMF, particularly polyester, is attributed to multifaceted market trends. Factors such as the increasing emphasis on fitness, characterized by a growing population engaging in sports and physical activities, spur a demand for activewear that seamlessly blends comfort and performance. Additionally, the ever-evolving fashion industry, with its short cycles and reliance on synthetic fibres like polyester, reflects a crucial linkage between fibre choice and market dynamics. Affordability and quality considerations further contribute to the rise of MMF, as polyester, costing half as much per kilo as cotton, offers functional properties like stretch, durability, and easy maintenance. Beyond market trends, environmental concerns and limitations of natural fibres, such as cotton, bolster the ascendancy of MMF. The unsustainable practices associated with cotton production, its vast land and water requirements, and the detrimental impact of pesticides prompt a reevaluation of fibre choices [1].

Despite the inherent advantages of MMF, especially in durability, water repellency, and ease of maintenance, the focus of this thesis extends to a critical aspect of thermal comfort. As literature underscores the complexities of moisture management in textiles, recent research emphasises the challenges faced by synthetic fibres like polyester and nylon in delivering optimal comfort compared to natural fibres. While these synthetic fibres excel in durability and affordability, moisture management remains a critical dimension where they often fall short of consumer expectations [2], [3]. This thesis delves into the engineering design of man-made fibrous textile structures, particularly focusing on polyester, to optimize wicking properties. It seeks to address the nuanced relationship between fibre structure and thermal comfort, exploring innovative approaches to enhance moisture management in synthetic textiles. By examining the latest techniques and innovations, this research aims to contribute to the ongoing discourse on achieving superior comfort in MMF textiles, positioning them as versatile and comfortable alternatives in diverse applications.

3 OBJECTIVES

Recognizing the pivotal role of man-made fibres (MMF) constituting a significant share of the textile market, and understanding the critical challenge associated with their lack of comfort properties, the objectives were designed to conduct a thorough investigation into fundamental principles and to optimize wicking properties in MMF textiles.

Objective 1: Conduct an extensive literature review on the fundamental principles and mechanisms that will govern liquid moisture management in Man-Made Fibrous (MMF) textiles.

Objective 2: Investigate innovative finishing techniques for enhancing moisture management in synthetic fabrics, with a focus on polyester and nylon. Explore state-of-the-art finishing processes addressing challenges related to wicking, absorbency, and moisture transport in synthetic fabrics.

Objective 3: Conduct a detailed investigation into the wicking behaviour of polyester filament yarns and fabrics, focusing on cross-section, deniers, textures, intermingling, and knit structures. Establish a correlation between filament yarn and fabric properties and the resulting wicking performance in fabrics, aiming to provide insights into achieving necessary wicking performance in both yarn and fabric development. Contribute valuable information for selecting optimal filament yarn characteristics to enhance vertical and horizontal wicking behaviour in knitted sportswear fabrics.

Objective 4: Thoroughly examine the wicking performance of polyester filament with the unique C-shape cross-section. Develop a theoretical model using mathematical equations to predict the wicking behaviour of C-shape cross-section polyester multifilament yarns with diverse packing densities. Validate the developed model by comparing its predictions with experimental data obtained from wicking tests on real polyester fabrics.

Objective 5: Develop a cost-effective instrument for the precise evaluation of horizontal wicking properties in fabrics, utilizing innovative image analysis.

A step-by-step approach is taken to address each goal. Existing research is delved into, practical experiments are conducted, the results are carefully analyzed, and the discoveries are shared in presentations and publications. This comprehensive approach ensures a deep understanding and effective resolution of challenges in enhancing the comfort of man-made fibrous textiles in terms of heat.

4 LITERATURE REVIEW

4.1 Developments in Fabric Structure for Enhancing Moisture Management Properties

Textile fabrics and their quality are steadily increasing in demand due to the rising living standards of consumers worldwide. Elevated levels of moisture management and comfort properties are now sought by users in both active wear and daily garments. Moisture management in fabrics is defined as the movement of water vapour and liquid moisture from the skin's surface to the fabric and from the fabric to the atmosphere through the garment worn by an individual. Several factors, such as the structural parameters of the fabrics, the type of fibre, fibre cross-section, yarn type, fabric weave, etc., have an impact on the comfort properties of the fabrics[4]. This chapter focuses on the fundamental principles and basic mechanisms involved in liquid moisture management, as well as recent developments in fibre structure aimed at enhancing moisture management properties.

4.1.1 The scientific principles underlying moisture-wicking in fabrics

Capillary action is facilitating the transfer of liquids through the microcavities of the yarn, driven by differential air pressure. This phenomenon, known as wicking, takes place when fibres exhibit hydrophilic characteristics, leading to the absorption of water by the fibres. On the other hand, wicking in hydrophobic fibres such as polyester is occurs without actual water absorption into the fibres [5]. The wicking capability of fabrics is of paramount importance in moisture absorbency and management, particularly in the case of hydrophobic textile fabrics. The ability of a fabric to support the capillary flow of liquid through inter-fibre or inter-yarn spaces is referred to as the wicking ability [6]. The wicking coefficient (A) is associated with micro capillaries or pore structure, the chemical composition of the fibre surface, and the characteristics of the liquid. The formula expressing the wicking coefficient is:

$$A = R\left[\frac{\gamma\, cos\theta}{2\eta}\right] \text{..... Equation 1}$$

In this context, R is represented by the radius of the micro-pores capillary, γ is denoted as the surface tension of the liquid, θ is the contact angle between the liquid and fibres, and η is referred to as the viscosity of the water/liquid[4], [7]. The combined moisture management properties of a fabric are influenced by both its absorbency and wicking ability [8].

Fabric wicking properties can be assessed through tests such as the vertical strip test, horizontal, or planner test [9]–[11]. Common wicking test methods are included in AATCC Test Method 79-2000,

197-2011, and 198-2011. The Gravimetric Absorbency Testing System (GATS) is used for evaluating the absorption capacity of fabric specimens.

The Moisture Management Tester (MMT) is a modern instrument used for measuring fabric liquid moisture management properties, offering wicking indices for both the fabric's top and bottom sides [12]. Following the planner wicking test principle, the MMT assesses fabric moisture transmission properties as per AATCC Test Method 195[13]. In this test, a fabric sample is positioned horizontally, with one side adjacent to the skin on top and the other side facing outward at the bottom of the testing instrument. The time taken to wet the top and bottom of the fabric is measured in seconds. The MMT evaluates absorption rate, spreading speed, maximum wetted radius, accumulative one-way transport capability, and overall moisture management capability, providing a comprehensive index of a fabric's ability to transport liquid [14].

4.1.2 Effect of Fibre Properties

The hydrophobic or hydrophilic character of textile fibres is determined by the presence of polar or non-polar groups. Water molecules are attracted by polar and non-polar groups, leading to water absorption into the fibres. The absence of such groups results in the hydrophobic nature of fibres. Water absorption within a fibre is influenced by its crystalline structure, crystallite size, orientation and distribution, as well as the presence and size of amorphous regions [15].

Low moisture absorption but efficient moisture transport is exhibited by hydrophobic fibres, like polyester, due to the limited bonding sites available for water binding. On the other hand, moisture absorption is excelled by hydrophilic fibres but they are less effective in moisture transfer and discharge, attributed to the presence of bonding sites for water molecules [16], [17]. Improved wicking and moisture management are demonstrated by fabrics structured with hydrophobic fibres having non-circular or profiled cross-sections compared to fabrics produced with fibres of round cross-sections[18], [19].

Superior wicking and moisture management are demonstrated by fabrics produced with micro-denier fibres compared to those made from higher-denier fibres [20]. Enhanced moisture management and a higher specific surface area for quicker drying are exhibited by yarns crafted from micro-denier fibres, featuring numerous micro capillaries. Improved moisture management in fabrics with fibrillated structures results from fibrillated fibres, featuring micro capillaries for moisture wicking and transportation [21], [22].

Enhanced moisture management properties are shown by blends of fibres compared to fabrics made from individual fibres. Improved moisture management is exhibited by blends such as wool and polyester, wool and bamboo, and cotton and bamboo compared to fabrics made from 100% cotton, bamboo, and wool [23]–[25].

4.1.3 Examples of Filament Yarns with Improved Comfort Performance

Exceptionally lightweight and fine microfibres like 'Trevira Finesse' and 'Fortel MicroSpun' are featured, offering a large specific surface area relative to their weight. Enhanced antistatic, high-stretch, and thermo-isolating properties in fabrics are exhibited by these very fine deniers, including high-performance microfibres and ultra-microfibres, making them both comfortable and highly functional [26]. Tri-lobal cross-sections characterize Tactel, a polyamide nylon 6-6 fibre from DuPont, and it is air-jet textured for a softer, more natural handle. Superior strength, elasticity, a soft feel, and good moisture management properties are offered by Tactel Micro and Supplex Micro, also from DuPont[27]. A lobed polyester fibre patented and manufactured by DuPont is Coolmax, featuring tetra-channel or hexa-channel cross-sections that act as drain capillaries, pulling moisture from the skin to the inner and outer layers of the fabric. Enhanced horizontal and vertical wicking abilities are achieved by the channelled cross-section structure, and fabrics made from Coolmax fibres dry faster due to a 20% larger surface area compared to conventional round polyester fibres [23]. VILOFT® is a viscose fibre with a flat cross-section and crenellated surface for improved wicking and quick-drying properties. Used to create functional fabrics for underwear, sportswear, formalwear, etc., VILOFT is blended with other natural and synthetic fibres. Different types of Viloft fibres, such as Viloft original and Viloft micro, offer similar aesthetic and handle properties as natural fibres with improved moisture and temperature management[28]. A polyester fibre by Toray Industries Inc. is Fieldsensor, which consists of a polyester filament yarn with grooves that help absorb sweat quickly and disperse perspiration throughout the fabric's outer surface for rapid vaporization [29]. Another polyester fibre, Coolpass®, features a tetra-lobed cross-section and micro slots on its longitudinal surface. The tetra-lobed cross-section allows for a closer arrangement of fibres, while micro slots act as capillaries to wick moisture [30]. Dri-release is a composite yarn comprising 85-90% hydrophobic fibres for wicking action and 10-15% hydrophilic fibres for moisture absorbency. Typically, it involves blending 85% polyester fibres with 15% cotton fibres. Natural fibres serve as moisture absorbers, drawing moisture away from the skin, while synthetic fibres repel moisture to the surface of the garment. Once on the garment's surface, moisture is

evaporated quickly upon contact with dry airflow. Due to the synthetic fibres' capacity to release moisture into the atmosphere, these yarns are termed Dri-release yarns, commonly utilized in athletic wear, socks, and underwear [31].

4.1.4 Summary:

The literature review on man-made fibre fabrics and their impact on moisture management unveils several advancements in fibre cross-section and surface design to enhance the moisture management properties of fabrics. In literature, some studies explore the blending of hydrophilic regenerated and natural fibres to enhance the moisture management capabilities of fabrics. The Micro and Nano fibres create a multitude of micro capillaries for effective wicking and offer a larger surface area for rapid drying.

4.2 Finishing Techniques for Improved Moisture Management

In the domain of textile engineering, the quest for enhancing moisture management properties in synthetic fabrics like polyester and nylon has spurred the development of innovative finishing processes. The challenges faced by these fabrics, particularly in wicking, absorbency, and moisture transport, delves into cutting-edge techniques designed to overcome these hurdles. The researchers are venturing into physical and chemical finishing processes that provide the desired level of thermal comfort to wearers.

4.2.1 Physical Finishing Processes: Modifying Fabric Structure for Enhanced Moisture Management

In the pursuit of improving moisture management properties in synthetic fabrics, a pivotal role is played by physical finishing processes in modifying the fabric's physical structure. Key examples of physical finishing processes include:

Calendaring: In this process, the fabric passes between heated rollers under pressure. Fibres are flattened, creating a more uniform surface that improves wicking and moisture evaporation properties. Calendaring reduces surface roughness, thereby enhancing the fabric's capability to effectively spread and evaporate moisture [32].

Plasma Treatment: This involves exposing the fabric to a plasma discharge, generating reactive chemical species that modify the surface properties of fibres. Plasma treatment creates a hydrophilic surface on the fabric, improving wicking and moisture absorption properties. By introducing polar groups onto the fibre surface, this process enhances the fabric's affinity for water molecules[33].

4.2.2 Chemical Finishing: Augmenting Hydrophilicity with Hydrophilic Agents

Enhancing moisture management properties in polyester and nylon fabrics by chemical finishing involves developing a charge on the fabric with cationization, and applying hydrophilic agents such as hydrophilic softeners and Wicking Agents to transfer moisture [2].

Cationization: In this process, the fabric is treated with a cationic agent, like quaternary ammonium compounds, providing the fabric with a positive charge. This positive charge attracts water molecules, enhancing the fabric's wicking and moisture absorption properties.

Application of Hydrophilic Polymers: Utilizing hydrophilic polymers such as polyethylene glycol (PEG) and polyvinyl alcohol (PVA) on the fabric's surface improves wettability and wicking properties. These substances, known for their strong affinity for water, alter the fabric's inherent hydrophobicity, rendering it more water-absorbent and moisture-wicking[34].

Application of Moisture Wicking Agents: Agents like N-methyl morpholine oxide (NMMO) can be applied to the fabric's surface to enhance its ability to transport moisture away from the skin. These agents can be incorporated into various finishing formulations, including resins, binders, and emulsions[35].

4.2.3 Smart Textiles: Adapting Fabrics to Environmental Conditions

The exploration of smart textiles stands as an exhilarating frontier within the landscape of moisture management research, introducing advanced materials and technologies that exhibit a capacity to sense, respond to, or adapt to prevailing environmental conditions.

Moisture-Sensing Fabrics for Personalized Comfort: Advancements in moisture-sensing fabrics are unfolding, marking progress in the development of materials designed to detect fluctuations in humidity and moisture levels. These fabrics possess the capability to signal when proactive moisture management is essential, ensuring wearers experience sustained comfort across diverse environmental settings.

Active Moisture Transport for Extreme Conditions: Smart textiles incorporating integrated microfluidic systems or electro-responsive materials engineered to transport moisture away from the body actively. Particularly in intense physical activity or hot and humid environments, these systems hold significant potential for revolutionizing moisture management dynamics.

4.2.4 Summary

Physical finishing processes, calendaring, and plasma treatment play a vital role in modifying fabric structure for enhanced moisture absorption and wicking. Chemical finishing methods, such as

cationization and the application of hydrophilic polymers and moisture-wicking agents, augment hydrophilicity and improve fabric comfort. Despite their effectiveness, chemical finishes may not provide a long-term solution. While these advancements offer solutions, it is emphasizes that physical modifications in fabric structure remain crucial for sustainable and long-lasting improvements in moisture management for synthetic fabrics.

5 CONTRIBUTION

5.1 Wicking Properties of Polyester Filament Yarns Used in Sportswear

Polyester filament yarns, integral to the production of sportswear fabrics, are sourced from the manmade fibre industries. The wicking performance of samples of these polyester filament yarns is delved into in this study, aiming to ascertain their respective wicking heights. Employing the capillary rise approach, the wicking properties of these yarns are systematically tested. The test results are scrutinized to explore the influences of filament cross-section, deniers per filament, textures, and intermingling on the observed wicking height.

5.1.1 Experimental Methods and Materials

Filament yarns are sourced from industrial sources to investigate the impact of filament yarn structure on wicking performance. Diverse filament cross-sections, varying deniers per filament, including flat yarn samples, textured yarns, and blends with Lycra filaments[27], [36], [37], are exhibited by these yarn samples. All these variants are found to be applied in sportswear fabrics, leveraging their distinct technical and performance attributes. The yarn wicking test involves vertically suspending a 25 cm long yarn sample, ensuring the filaments remain straight by applying a 5 gm mass at the bottom [38], [39]. The vertical wicking height for all three samples is systematically measured over time utilizing a vertical wicking tester. The entire process, spanning from the initiation of the wicking process to the establishment of equilibrium in the yarn, is meticulously documented. To enhance visual clarity and facilitate observation of the flow, water is augmented with 3 g/l blue reactive dye, serving as a tracer for the experiment. This dye addition aids in improving the visibility of the wicking process dynamics [40]. This meticulous testing methodology ensures reliable and accurate assessments of the wicking properties of filament yarns, contributing to a comprehensive understanding of their moisture management characteristics.

5.1.2 Results and Discussion:

Details of the filament yarns and corresponding test results are comprehensively presented in Table 1. Vital information on various parameters, including filament cross-sections, deniers per filament, textures, and intermingling, is encapsulated by the table, shedding light on their influence on wicking performance.

Table 5.1: Wicking test results of the yarn samples.

Sample ID	Yarn Denier	Number of Filament	Denier per filament	Filament Cross Section	Type of Filament	Wicking Height in cm		
						5 Min	10 Min	15 Min
A	75	36	2.1	Triangular	FDY	2.4	4	4.5
B	100	36	2.8	Triangular	FDY	2.8	4.4	5.1
C	75	36	2.1	Circular	FDY	1.9	3.2	4.1
D	100	36	2.8	Circular	FDY	1.5	2.8	3.4
E	100	72	1.4	Circular	FDY	3.3	4.3	5.5
F	150	96	1.6	Circular	FDY	2.9	3.7	4.7
G	100	72	1.4	Circular	BCF	3.5	4.5	5.8
H	150	96	1.6	Circular	BCF	3.1	4.4	5.7
I	80	108	0.7	Circular	DTY MICRO	3.8	4.8	6.1
J	80	48	1.7	Circular	DTY	3.3	4.2	5.4
K	75	36	2.1	Circular	DTY	2.2	3.7	4.4
L	100	36	2.8	Circular	DTY	1.8	3.2	3.9
M	75+20	36	2.1	Circular	HIM 20 D	2.8	4.1	4.8
N	100+20	36	2.8	Circular	HIM 20 D	2.1	3.6	4.2

5.1.2.1 Effect of Filament Denier on Yarn Wicking Performance

Observations reveal that, across all time intervals, superior wicking is consistently demonstrated by finer filaments compared to coarser counterparts. In finer denier filaments, a more linear increase in wicking height over time is exhibited, contrasting with coarser denier filaments where the rise in wicking height diminishes after the initial 10 minutes.

Moreover, a notable influence of denier on dynamic wicking behaviour, particularly evident in textured yarns, is demonstrated through the evaluation of wicking properties among bulk continuous filaments and textured yarn samples.

5.1.2.2 Effect of Filament Cross Section on Yarn Wicking Properties

The wicking characteristics of circular and triangular filament yarns, varying in denier within fully drawn polyester filament yarn, reveal that greater wicking heights are exhibited by triangular filament yarns compared to circular filament yarns of the same denier.

5.1.2.3 Effect of Texturing on the Wicking Property of Yarns

Observations from the wicking behaviour of polyester filament yarns, including fully drawn, drawn textured, and bulk continuous filament yarn, reveal that higher wicking heights are exhibited by drawn textured yarn and bulk continuous filament yarn compared to the fully drawn yarn of the same denier per filament. Consequently, texturing influences yarn-wicking properties, in addition to denier per filament. The structural disparity between textured yarn and parallel-drawn yarn is well-established, where fully drawn yarn filaments align parallelly, while textured yarn features filaments with numerous curls and pores, resulting in a bulkier yarn with increased capillary effectiveness.

5.1.2.4 Effect of Lycra Intermingling on the Wicking Property of Yarns

Utilizing intermingling as an alternative method to enhance filament yarn resistance against high-volume stress has emerged as an effective replacement for traditional approaches like sizing and twisting, contributing to the durability of filament yarns. The intermingling effect on draw-textured polyester filament yarn's wicking height reveals that, in comparison with the parent draw-textured yarn, the intermingled yarn demonstrates a higher wicking height. The combination of a compact and closely continuous structure generates water reservoirs and open spaces within the yarn, facilitating capillary action to distribute water effectively.

5.1.3 Summary

In this chapter, the wicking behaviour of various commercial polyester filament yarns, specifically designed for sportswear, is examined using a capillary rise test. The key findings derived from the test results can be summarized as follows: Firstly, the wicking height decreases as filament denier increases, observed in both fully drawn and textured yarns. Additionally, triangular cross-section filaments exhibit superior wicking heights when compared to circular ones, especially notable in coarser denier filaments with enhanced wicking performance. Moreover, textured draw and continuous bulk filament yarns show heightened wicking heights in comparison to fully drawn yarns. Lastly, the application of intermingling processes contributes to elevated wicking heights in draw-textured yarns.

5.2 Wicking Properties of Polyester Filament Yarn Knitted Fabrics Used in Sportswear

The hydrophobic nature of traditional polyester, along with its limited thermal transfer capacity, hinders its extensive use in summer and sportswear fabrics. In contrast, nylon fibres, with their moisture-sensitive characteristics and enhanced thermal transfer properties[41], [42], offer a viable

alternative. This chapter thoroughly investigates the influence of knitted fabric structures, Single jersey, Lock knit, Matty, and Crepe on both vertical and horizontal wicking behaviours. All four fabric samples are developed using 100 denier draw-textured polyester filament yarns with 36 filaments.

5.2.1 Experimental Methods and Materials

In pursuit of enhancing the water transport properties of Draw Textured Filament Yarns, four knit structures, Single jersey, Lock knit, Matty, and Crepe were manufactured using polyester DTY 100 Denier with 36 filaments. These fabrics, aimed at achieving 150-160 GSM, encompass specific details regarding fabric structure and obtained actual GSM.

Vertical Wicking: Fabric specimens (200mm × 25mm) were prepared along wales-wise and course-wise directions, suspended vertically with their bottom ends immersed in distilled water. Wicking height, the distance travelled by water on the vertical strip, was measured at one-minute intervals for 20 minutes [43].

Horizontal Wicking: Fabric samples were mounted on an embroidery frame, and a micropipette was used to place a drop (50 mL) of water on the fabric. The area spread in 1 minute was measured manually for both the face and back sides. The average of both face and back side horizontal wicking was considered as the wicking area of the fabric. The blue colour added to water facilitated visual tracking of water movement during wicking [44].

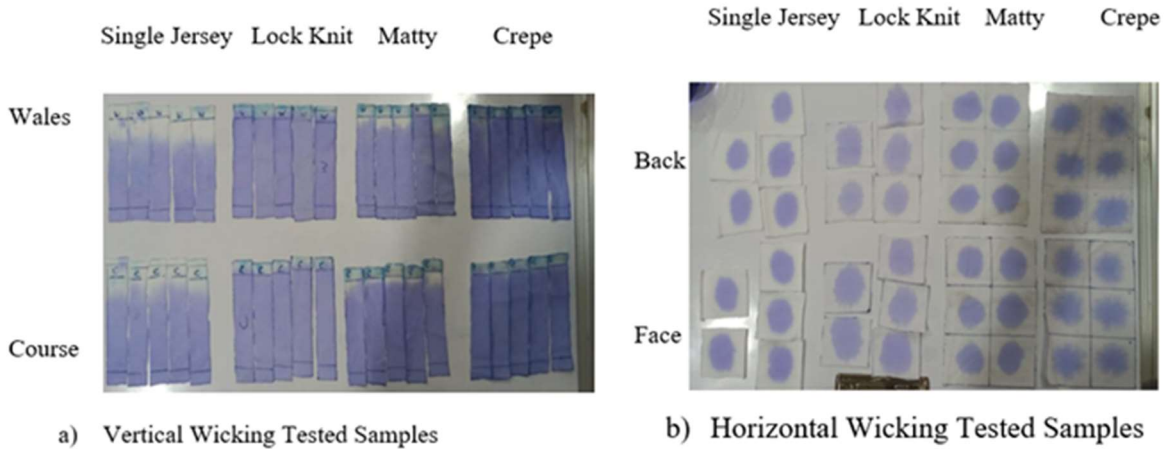

Figure 5.1: Fabric samples tested for wicking

Fabric-wicking experiments were conducted in a standard atmosphere (20 ± 2°C, 65 ± 2% relative humidity) with a 24-hour fabric conditioning period. To minimize test errors, five samples of each

type were tested for vertical and horizontal wicking, with the average result representing the fabric's wicking property, as depicted in Figure 5.1.

5.2.2 Results and Discussion

The study focused on assessing the vertical and horizontal wicking capacities of knitted fabrics, taking into account variations in knitted structure, Courses and Wales per inch and loop length. Table 5.2 details the vertical wicking height in both course and wale directions, whereas Table 5.3 showcases the horizontal wicking area in mm square of four fabric structures, all manufactured using 100 denier polyester draw-textured yarn.

Table 5.2: Vertical wicking in wale and course direction

	Vertical Wicking Height in cm Wale direction of knitted fabric structures				**Vertical Wicking Height in cm Course direction of knitted fabric structures**			
Time in Minute	**Single Jersey**	**Lock Knit**	**Matty**	**Crepe**	**Single Jersey**	**Lock Knit**	**Matty**	**Crepe**
1	4.5	4.6	2.9	2.6	4.5	4.5	2.8	2.5
2	4.7	4.9	3.6	3.7	4.8	4.8	3.5	3.5
3	4.9	5.4	4.1	4.5	5	5.2	4.2	4.3
4	5.1	5.8	4.7	4.9	5.2	5.6	4.6	4.7
5	5.3	6.2	5.8	5.2	5.4	6.1	5.5	5
6	5.5	6.5	6	5.7	5.7	6.4	5.9	5.5
7	5.7	6.8	6.2	6.1	5.9	6.7	6.3	5.9
8	5.9	7.1	6.4	6.4	6	6.9	6.5	6.3
9	6.1	7.3	6.6	6.8	6.1	7.2	6.7	6.5
10	6.2	7.5	6.8	7	6.2	7.5	6.8	6.9
11	6.3	7.7	6.9	7.2	6.3	7.7	7	7.1
12	6.4	7.9	7	7.4	6.4	7.9	7.1	7.3
13	6.4	8.1	7.1	7.6	6.5	8.1	7.2	7.4
14	6.5	8.3	7.3	7.8	6.6	8.2	7.3	7.6
15	6.5	8.4	7.4	7.9	6.7	8.3	7.4	7.8
16	6.6	8.5	7.5	8	6.8	8.4	7.5	8
17	6.6	8.6	7.6	8.2	6.8	8.4	7.6	8.2
18	6.7	8.7	7.8	8.2	6.9	8.5	7.8	8.2
19	6.7	8.8	7.8	8.3	6.9	8.5	7.8	8.3
20	6.7	8.8	7.8	8.3	6.9	8.5	7.9	8.1

5.2.2.1 Vertical Wicking in Wale Direction:

Single Jersey and Lock Knit Dominance: Single Jersey and Lock Knit structures consistently outperform Matty and Crepe structures in wicking height throughout the test. This indicates that, in the wale direction, Single Jersey and Lock Knit fabrics exhibit superior water absorption characteristics.

Early Advantage for Single Jersey and Lock Knit: Single Jersey and Lock Knit structures show higher wicking heights right from the first minute. The initial advantage of Single Jersey and Lock Knit over Matty and Crepe structures is pronounced in the early stages of the test.

Matty and Crepe Catch-Up: While Matty and Crepe structures start with lower wicking heights, they demonstrate a more rapid increase over time. After 5 minutes, the wicking height in Matty and Crepe fabrics catches up with, and in some instances surpasses, that of Lock Knit and Single Jersey fabrics.

Flattening of the Curve: After 14-16 minutes, the wicking height curve for all fabric structures becomes relatively flat, indicating a minimal increase in wicking height. This suggests that, beyond a certain duration, the fabrics reach a saturation point in terms of water absorption.

5.2.2.2 Vertical Wicking in Course Direction:

Early Superiority for Single Jersey and Lock Knit: Similar to the wale direction, Single Jersey and Lock Knit structures demonstrate higher wicking heights in the course direction from the beginning of the test.

Matty and Crepe Overtake: In contrast to the wale direction, Matty and Crepe structures exhibit a more pronounced catch-up in the course direction. After 10 minutes, the wicking height in Matty and Crepe fabrics surpasses that of Single Jersey, indicating a reversal in performance over time.

Flattening of the Curve: As observed in the wale direction, the wicking height curve flattens for all fabric structures after 14-16 minutes, indicating saturation and minimal further increase.

Table 5.3: Horizontal wicking area in mm^2 after 1 minute

	Horizontal Wicking Area in mm^2 After 1 Minute		
Sr. No	**Face side**	**Back side**	**Average of Face and backside**
Single Jersey	725	672	698.5
Lock Knit	1022	946	984
Matty	813	804	808.5
Crepe	759	955	857

From the results presented in Table 5.3, we can derive a comparison of the horizontal wicking performance among different knit structures after 1 minute. The average horizontal wicking areas are as follows:

Lock Knit (984 mm2): Lock Knit demonstrates the highest average horizontal wicking area after 1 minute, indicating superior initial water absorption compared to other knit structures.

Matty (808.5 mm2): Matty follows closely behind Lock Knit, exhibiting a substantial horizontal wicking area after 1 minute.

Single Jersey (698.5 mm2): Single Jersey shows a moderate average horizontal wicking area, suggesting a reasonable level of water absorption in the initial phase.

Crepe (857 mm2): Crepe lags behind Lock Knit and Matty but still exhibits a notable horizontal wicking area after 1 minute.

The comparison reveals that Lock Knit outperforms the other knit structures in terms of horizontal wicking performance at the early stage of the test. Matty also shows strong initial performance, while Single Jersey and Crepe exhibit moderate and decent horizontal wicking, respectively.

5.2.3 Summary

The study on the wicking properties of polyester filament yarn knitted fabrics used in sportswear sheds light on the critical influence of fabric structure on water absorption. Single Jersey and Lock Knit structures exhibit consistent dominance in both vertical and horizontal wicking, particularly in the wale direction. Their early advantage suggests superior water absorption characteristics, although Matty and Crepe structures catch up over time. The flattening of the wicking height curve after 14-16 minutes indicates a saturation point in water absorption for all fabric structures. This comprehensive analysis provides valuable insights for fabric selection in sportswear, emphasizing the need for a balanced approach considering instant wicking capabilities and sustained performance over time.

5.3 Wicking Performance of C-Shape Filament Yarn for Comfort Fabrics

This chapter delves into the profound impact of fibre choice on the wearer's comfort, with a specific focus on the wicking performance of the polyester fabric. The investigation scrutinizes the distinctive influence of C-shaped cross-section filament yarn compared to circular cross-section filament yarn. Experimental findings shed light on the superior wicking capabilities of C-shaped filaments, attributing this enhancement to the increased surface area facilitating capillary action and

the formation of micro and linear capillaries within the unique C-shaped cross-section of the filament.

5.3.1 Experimental Methods and Materials

To experimentally validate the proposed mathematical model for polyester filament yarn with C-shape cross-sections, circular and C-shape filament yarns were fabricated at the Bombay Textile Research Association lab using a melt spinning machine.

5.3.1.1 Manufacturing Filament Yarns with Varied Cross-Sections

The manufacturing process involved the use of a melt-spinning machine manufactured by Textile Equipment Co. in Delhi. During the process, the spinning temperature was maintained at 220°C. Subsequently, the drawing temperatures of the three heaters or drawing rollers were precisely controlled at 180°C, 190°C, and 200°C. These specific temperature settings across the heating zones ensured the controlled and efficient formation of filament yarn with circular and C-shaped cross-sections. The strategic manipulation of temperature parameters is crucial in determining the physical characteristics of the resulting filaments, influencing their dimensions and cross-sectional shapes.

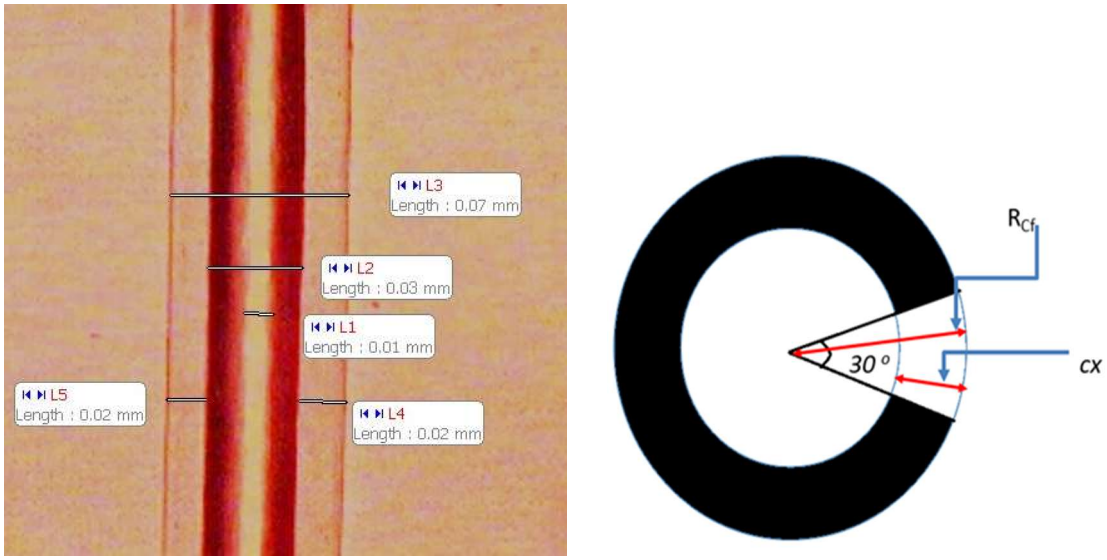

Figure 5.2: Microscopic image of the C-shape filament yarn

5.3.1.2 Microscopic Analysis of Filament Characteristics

Utilizing a microscope, circular and C-shaped filaments were meticulously examined at ten different locations for each specimen, and the average dimensions are summarized in Table 5.4. The yarn samples underwent thorough inspection using an electronic microscope to determine filament

diameter and cross-section shape. Figure 5.2 provides a reference microscopic image of the C-shaped filament yarn. The cross-sections of C-shaped filaments showcase a distinctive hollow open cavity, defining their classification as C-shape cross-sections. In contrast, filaments with round cross-sections display solid and uniform circular profiles.

Table 5.4: Dimensions of Circular and C-Shaped filament yarns

Circular Cross-section Filaments			**C Shape Cross-section Filaments**					
	Number of Filaments	**Diameter**		**Number of Filaments**	**Outer Diameter**	**Inner Diameter**	**θc**	**Thickness of C Curve**
Sample 1	36	0.07 mm	**Sample 5**	36	0.07 mm	0.03 mm	30º	0.02 mm
Sample 2	36	0.09 mm	**Sample 6**	36	0.09 mm	0.03 mm	30º	0.03 mm
Sample 3	36	0.11 mm	**Sample 7**	36	0.11 mm	0.04 mm	30º	0.035 mm
Sample 4	36	0.13 mm	**Sample 8**	36	0.13 mm	0.05 mm	30º	0.04 mm

5.3.1.3 Experimental Determination of Vertical Wicking Height

The vertical wicking height for all three samples was systematically measured over time utilizing a vertical wicking tester. The entire process, spanning from the initiation of the wicking process to the establishment of equilibrium in the yarn, was meticulously documented. To enhance visual clarity and facilitate observation of the flow, water was augmented with 3 g/l blue reactive dye, serving as a tracer for the experiment. This dye addition aids in improving the visibility of the wicking process dynamics [40].

5.3.2 Results and Discussion

This study meticulously compared the maximum wicking heights achieved by circular and C-shaped filament yarns. The ensuing test results, presented in Table 5.5 and 5.6, provide a thorough understanding of the wicking performance exhibited by Circular Cross Section Filament Yarns and C-shaped cross-section Filament Yarns.

Table 5.5: Maximum wicking height of Circular cross-section filament yarns

	Number of Filaments	**Diameter (mm)**	**Experimental Maximum Wicking Height (mm)**
Sample 1	36	0.07	58
Sample 2	36	0.09	51
Sample 3	36	0.11	40
Sample 4	36	0.13	35

Table 5.6: Maximum wicking height of C-Shape cross-section filament yarns

	Outer Diameter (mm)	**Inner Diameter (mm)**	**Experimental Maximum Wicking Height (mm)**

Sample 5	0.07 mm	0.03 mm	77
Sample 6	0.09 mm	0.03 mm	65
Sample 7	0.11 mm	0.04 mm	57
Sample 8	0.13 mm	0.05 mm	45

The wicking performance of Circular Cross Section Filament Yarns was assessed through variations in filament diameter, with Sample 1 exhibiting a diameter of 0.07 mm and achieving the highest wicking height of 58 mm. As the diameter increased in subsequent samples, the corresponding wicking heights showed a decreasing trend. This suggests that, in the case of circular filaments, a finer diameter contributes to enhanced wicking capabilities. Conversely, C-shaped cross-section filaments, as depicted in Table 5.6, demonstrated superior wicking abilities compared to their circular counterparts. Sample 5, featuring the smallest outer diameter (0.07 mm) and inner diameter (0.03 mm), outperformed all other samples with a remarkable maximum wicking height of 77 mm. The unique C-shaped structure, creating additional surface area for capillary action and forming micro and linear capillaries, contributed to the enhanced wicking performance observed across all samples.

5.3.3 Summary

The experimental findings affirm that C-shaped cross-section filament yarns exhibit superior wicking performance when compared to Circular Cross Section Filament Yarns. The distinctive structural attributes of C-shaped filaments, promoting efficient moisture dispersion, make them promising candidates for comfort fabrics in sportswear and activewear applications. The increased surface area and capillary structures within the C shape contribute significantly to the observed higher wicking heights, emphasizing the potential of this filament yarn design for optimizing moisture management in textiles. Mathematical Models for C Shape Filament Yarn Wicking

The primary focus is on unravelling the wicking behaviour inherent in multifilament yarns featuring a unique C-shaped cross-section. Drawing inspiration from circular yarn equations, our research seamlessly integrates theoretical models, aligning them with experiments conducted on polyester filament yarns, as detailed in Chapter 5.3 and sourced from the Bombay Textile Research Association (BTRA) Lab. The study meticulously examines crucial parameters, including filament cross-sectional shape, diameter, packing, and filament-water contact angle. Experimental verification solidifies the precision of our developed model in predicting the maximum wicking height over time. This work lays a robust foundation for a comprehensive understanding of wicking

behaviours and provides valuable insights for optimizing filament yarn designs to enhance overall performance.

5.3.4 Nomenclature

P_C Capillary pressure (dyne/cm^2)

r Radius of the capillary (cm)

γ_{LV} Surface tension between liquid and vapour interface (dyne/cm)- 72.5 dynes/cm

θ Water to Polyester Contact angle- 105 ^{o}

ρ Density of liquid (g/c.c.) – 1 g/c.c.

g Gravitational acceleration =981 cm /s^2.

ΔP Pressure difference

η Viscosity of the water - 8.90 × 10−3 dyne. second /cm^2

h Yarn wicking height (cm)

h_{max} Equilibrium capillary height (cm)

t Time of wicking (s)

5.3.4.1 For filaments with circular cross-section

μ Yarn packing co-efficient

R Radius of filament (cm)

a Distance between the nearest filaments' axis (cm)

x Distance between two filaments (cm)

D_H Hydraulic diameter of the capillary (cm)

5.3.4.2 For filaments with C-shaped cross-section

μ_C Yarn packing co-efficient

R_{Cf} Radius of outer curvature (cm)

r_{Cf} Radius of Inner curvature (cm)

C_x Thickness of C Shaped filament

a Distance between the nearest filaments' axis (cm)

x Distance between two filaments (cm)

D_{CH} Hydraulic diameter of the capillary (cm) pore formed with neighbouring filaments

D_{CCH} Hydraulic diameter of capillary (cm) pore formed within the C shape filament.

θ_C Angle of opening in C Shape filaments

5.3.5 Capillarity and Porous Yarn Structure

In scientific terminology, capillary action denotes the macroscopic movement or flow of a liquid influenced by its surface and interfacial forces. The wetting of filaments triggers liquid penetration into inter-filament spaces, inducing capillary pressure. Within narrow pore confines, this pressure compels the liquid to move along the capillary[45], [46]. Flowing liquid and wicking phenomena result from pressure differentials or capillary action [47]. The Laplace equation (Equation 2) quantifies the magnitude of capillary pressure:

$$P_c = \frac{2\pi r \gamma_{LV} \cos\theta}{\pi r^2} \quad \text{..... Equation 2}$$

The Hagen–Poiseuille law, governing laminar flow within a circular tube, is applied to an idealized tube structure, expressed y the folloing equaton:

$$Q = \frac{r^2}{8\eta} X \frac{\triangle P}{h} \text{..... Equation 3}$$

Additionally, this equation can also be used for steady-state flow through a porous medium [37]. In such cases, the hydraulic diameter of the pores is taken into account when defining pore diameter based on non-circularity and irregularity in the pore structure and spacing. The capillary rise was calculated from the Lukas-Washburn Equation as derived from the initial contact to equilibrium time [48].

$$ln\left(1 - \frac{h}{h_{max}}\right)^{-1} - \frac{h}{h_{max}} = Ct \text{..... Equation 4}$$

Where C is constant, at low values of t, h is very small comparative to the h_{max}, To establish the direct relationship between wicking height (h) and wicking time (t), the above equation is approximated as follows.

$$h = \sqrt{\frac{r\gamma_{LV} \cos\theta}{2\eta} Xt} \text{..... Equation 5}$$

This equation, rooted in the unique structure of textile yarns, emphasizes open channel capillaries formed by filament walls rather than conventional capillaries [49]. The challenge lies in modelling the intricate flow through textile structures due to the myriad variables and irregular capillary structures.

5.3.6 Mathematical Model Development

Our mathematical model integrates the Laplace and Hagen–Poiseuille equations, recognizing yarn as a porous material with embedded filaments and air. The capillaries within the yarn are depicted as open channels surrounded by filament walls, where the packing coefficient influences the proportion of the wall to the channel. Gravity acts as a resistance force against the flow through the channel.

The model unfolds in two key stages: first, the calculation of capillary flow, and second, the definition of pore geometry for both circular and C-shaped filaments. This dual-stage approach allows us to comprehensively capture the complex dynamics of vertical wicking in C-shaped filament yarns.

5.3.6.1 Step 1- capillary flow calculation

The assessment of capillary pressure entails two distinct methodologies. In Strategy 1, a singular pore (dimensionally) is utilized, where fictitious borders between pores demarcate each unit. The count and dimensions of pores are derived from prior computations. In Strategy 2, the entire pool of pores is treated as a cohesive porous system, with no consideration for imaginary boundaries between individual pores. Capillary pressure is computed using the total capillary force and the overall capillary area within the yarn [38].

For precision, the present study adopts Strategy 1, aligning with literature that asserts its superior accuracy compared to Strategy 2[36]. During vertical capillary flow through a capillary channel, two opposing forces come into play: the upward capillary force and the downward gravimetric force. The resulting pressure difference (ΔP) is expressed as: $\Delta P = \frac{2\pi r \gamma_{LV} \cos}{\pi r^2} - \frac{mg}{\pi r^2}$..... Equation 6

$$Pc = \frac{2\pi r \gamma_{LV} \cos\theta}{\pi r^2} \quad \text{Capillary force}$$

$$h\rho g = \frac{mg}{\pi r^2} = \quad \text{Gravimetric force}$$

$\Delta P = (Pc - h\rho g)$..... Equation 7

Here, ΔP signifies the pressure difference, ρ is the liquid density, m is the liquid mass wicked along the channel, and g is the gravitational acceleration. At maximum wicking high (h_{max}), the capillary pressure ΔP will be zero.

$$h_{max} = \frac{P_c}{\rho g}$$

$$h_{max} = \frac{\frac{2\pi r\gamma_{LV}\cos\theta}{\pi r^2}}{\rho g}$$

$$h_{max} = \frac{\frac{2\gamma_{LV}\,co}{r}}{\rho g}$$ ..... Equation 8

Substituting r with $D_H/2$, (Where D_H is the diameter of the capillary), the expression becomes

$$h_{max} = \frac{\frac{2\gamma_{LV}\cos\theta}{\frac{D_H}{2}}}{\rho g} = \frac{4\gamma_{LV}\cos\theta}{D_H\rho g}$$ ..... Equation 9

Equation (9) represents the maximum wicking height in the yarn, dependent on the hydraulic pore diameter D_H, which, in turn, relies on the filament structure and its arrangement within the yarn body.

5.3.6.2 Step 2- Defining Pore Geometry for Circular Filament Yarn

In the initial phase of establishing pore geometry for circular filament yarn, we rely on visual representations as detailed in Figure 1. The following foundational assumptions guide our approach:

- *The filaments within the yarn are hexagonally packed.*
- *All filaments possess identical dimensions.*
- *The spacing between all filaments is uniform.*
- *The cross-section of the filaments is circular.*

The capillaries formed between filaments in textile materials are open channels, created by the filament walls. In open-packed yarn, these capillaries can be represented by distinctly separating the actual filament border from the hypothetical border, as indicated in figure 5.4. The count of capillaries in an open-packed yarn matches that in a close-packed yarn, and the perimeter of the solid surface remains consistent. Figure 5.4 also illustrates the geometrical pore dimensions, showcasing variations only in the pore area and the perimeter, representing the imaginary boundary of a single capillary.

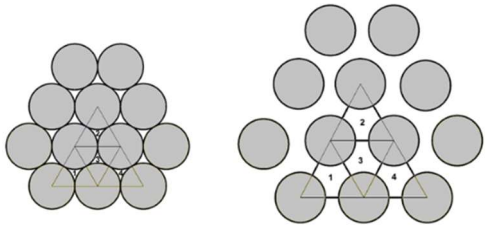

a) Close Packing b) Open Packing

Figure 5.3: Pore structure in hexagonally packed yarn (Das et al. 2011).

In Figure 5.5 a, the illustration depicts the region occupied by filaments, consisting of three sectors, each spanning 60 degrees of a circular cross-section. This area is situated within the unit yarn area, forming an equilateral triangle as illustrated in Figure 5.5 b, where the side length is denoted as 'a'. The combined area of the three sectors, each subtending 60 degrees, is equivalent to half the area of the circular filament cross-section, as depicted in Figure 5.5 c. This arrangement vividly showcases how the triangular yarn unit, with hexagonally arranged filaments, accommodates these specific circular sectors within its structure [38].

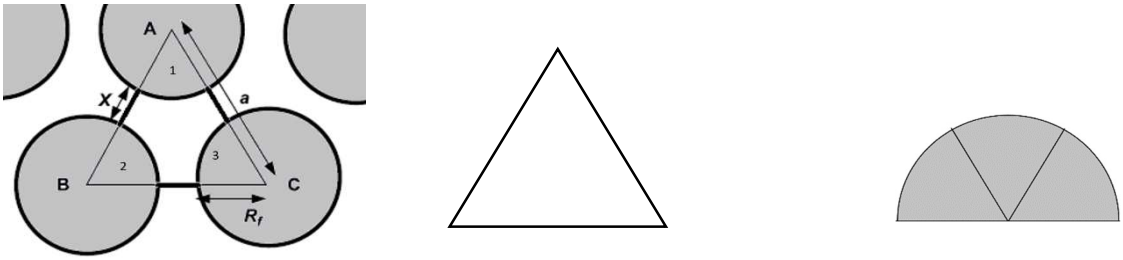

a) b) c)

Figure 5.4: a) Packing of filament in Yarn b) Unit area of yarn c) Area occupied by the filament

So the area of pore or capillary for weaking "A_p"

$(A_p) =$ Area of the triangle with side a – Area of Filament Sectors

$$= \frac{\sqrt{3}}{4} \times a^2 - \frac{\pi {R_f}^2}{2} \text{..... Equation 10}$$

The capillary pore diameter $D_H = 2\sqrt{\frac{A_p}{\pi}} = 2\sqrt{\frac{\frac{\sqrt{3}}{4} \times a^2 - \frac{\pi {R_f}^2}{2}}{\pi}}$

Where, D_H is the hydraulic diameter of the pore for circular filament yarn.

By employing Equation 9 and substituting the value of D_H , the maximum wicking height for the C-shaped filament yarn is determined.

5.3.6.3 Step 3- Defining Pore Geometry for C-Shaped Profile Filament Yarn

In defining the pore geometry for C-shaped profile filament yarn, several assumptions form the basis of the model:

- *The filaments within the yarn are hexagonally packed.*
- *All filaments possess identical dimensions.*
- *The spacing between all filaments is uniform.*
- *The cross-section of the filaments is C-shaped.*

This consideration aligns with the C-shaped profile of the filaments used in developing the mathematical model, as depicted in Figure 5.6. The organization of filaments within the yarn is modeled as hexagonal, mirroring the arrangement of circular filaments previously elucidated and depicted in Figure 5.7. In Figure 5.7 a, the geometric arrangement of filaments in yarn dimensions is illustrated. Meanwhile, Figure 5.7 b showcases the unit area of the yarn occupied by three C-shaped filaments with open cavities. Given the variance in filament profile from circular to C Shape, the pore diameter for C Shape filaments is expected to be greater than that for circular filaments.

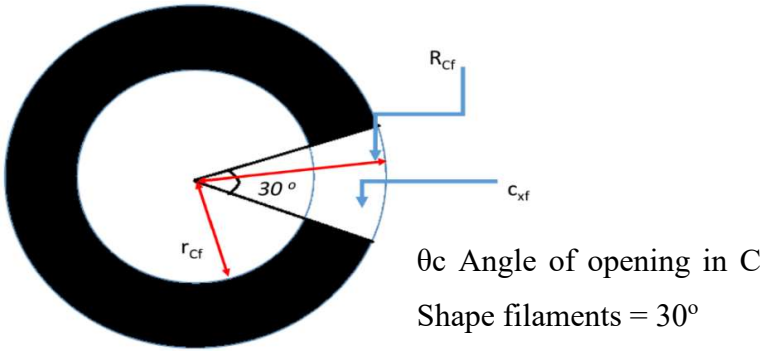

Figure 5.5: Structure of C-shaped filament used for calculating area occupied by filament.

This discrepancy arises due to the presence of a hollow cavity within the C Shape filament profile. In figure 5.8 a, the area occupied by the circular filament in the unit yarn space comprises three sectors, each of 60 degrees. In contrast, the area occupied by the C-shape filament is less than that of the circular filament due to the internal cavity and opening, as depicted in Figure 5.8 b with the shaded portion. The region occupied by the C-shape filament in the unit yarn space is determined by subtracting the area of three sectors, each of 60 degrees and diameter r_{Cf} from the area of three sectors, each of 60 degrees, with diameter R_{Cf}.

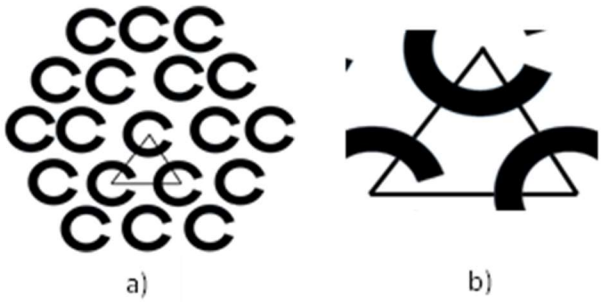

Figure 5.7: a) Geometrical arrangement of filaments in Yarn b) Unit area of Yarn.

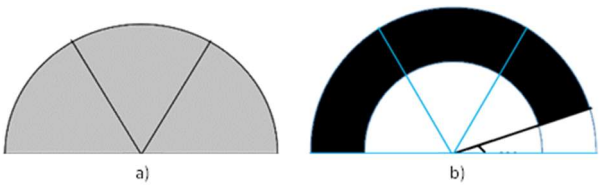

Figure 5.8: Area occupied by the a) Circular filament and b) C Shape filament.

Moreover, the computation includes deducting half the area of the sector with a 30-degree angle from the outer diameter while adding half the area of the sector with a 30-degree angle from the inner diameter. The area occupied by the C-shape filament in the unit yarn is calculated using the formula:

$$= \frac{\pi {R_f}^2}{2} - \frac{\pi {r_f}^2}{2} - \left(\frac{1}{2} \times \frac{30}{360}\frac{\pi {R_f}^2}{} - \frac{1}{2} \times \frac{30}{360}\frac{\pi {r_f}^2}{}\right)$$

$$= \frac{\pi {R_f}^2}{2} - \frac{\pi {r_f}^2}{2} - \left(\frac{1}{24}\frac{\pi {R_f}^2}{} - \frac{1}{24}\frac{\pi {r_f}^2}{}\right)$$

$$= \frac{\pi}{2}\left({R_f}^2 - {r_f}^2 - \frac{1}{12}{R_f}^2 + \frac{1}{12}{r_f}^2\right)$$

Therefore, the area of the pore or capillary for wicking in C-shape filament $(A_{cp})$is given by:

$=$ Area of the Trangle with side a – Area of C Shape Filament Sectors

$$A_{cp} = \frac{\sqrt{3}}{4} \times a^2 - \frac{\pi}{2}\left({R_f}^2 - {r_f}^2 - \frac{1}{12}{R_f}^2 + \frac{1}{12}{r_f}^2\right)$$

Thus, the hydraulic pore diameter D_{CH} for C-shape filament yarn is derived as follows:

$$D_{CH} = 2\sqrt{\frac{A_{Cp}}{\pi}} = 2\sqrt{\frac{\frac{\sqrt{3}}{4} \times a^2 - \frac{\pi}{2}\left({R_f}^2 - {r_f}^2 - \frac{1}{12}{R_f}^2 + \frac{1}{12}{r_f}^2\right)}{\pi}}$$

Using equation number 9 and putting a value o D_{CH}, instead of D_H, the maximum wicking height for the C shape filament yarn is calculated.

5.3.6.4 Step 4- Defining Pore Geometry by Accounting for the Cavity in C-Shape Profile Filament as the Pore

In step 3, the hydraulic diameter of the pore for wicking action is calculated by considering both the gap between the filaments and the open cavity formed in the C Shape filaments. Moving on to step 4, the hydraulic diameter (D_{CCH}) of the pore for wicking action is solely considered as the open cavity formed in the C-shaped filament. Since wicking height is inversely proportional to the diameter of the capillary, the size of the open cavity in the C-shaped filament is substantially smaller than the size of the pore formed between the filaments, especially when the filaments are not closely packed. The hydraulic pore diameter D_{CCH} of samples 5 to 8 is measured under an electronic microscope. Once again, using equation number 6 and substituting the value of " D_{CCH} " instead of " D_H " the maximum wicking height for the C shape filament yarn is calculated.

5.3.7 Experimental Methods and Materials

In the present chapter, 5.4 Mathematical Models for C Shape Filament Yarn Wicking, it is essential to note that the experimental materials and methods remain consistent with those detailed in Chapter 5.3. The samples and wicking test procedures discussed in the previous chapter serve as the foundation for validating the mathematical models presented here.

5.3.8 Results and Discussion

The study involves a comprehensive comparison of the maximum wicking heights between circular and C-shaped filament yarns, utilizing both theoretical predictions based on input parameters of filaments and yarns and experimental values. The primary objective is to analyze and compare the maximum wicking height values achieved through these two approaches. The detailed results are presented in Tables 5.7 and 5.8. Table 5.7 provides a comparative overview of the maximum wicking height values for Circular Cross Section Filament Yarns, while Table 5.8 offers a similar comparison for C-shaped cross-section Filament Yarns, presenting values derived from both experimental observations and the theoretical model.

Table 5.7. Maximum wicking height of Circular cross-section filament yarns.

	Number of Filaments	Diameter (mm)	Experimental Maximum Wicking Height (mm)	Theoretical Maximum Wicking height (mm)
Sample 1	36	0.07	58	61.78
Sample 2	36	0.09	51	53.71
Sample 3	36	0.11	40	42.32
Sample 4	36	0.13	35	38.46

The experimental results indicate that there is a close agreement between the calculated and observed maximum wicking heights for all tested samples. This alignment strengthens the validity of our theoretical model and suggests that our mathematical approach adequately captures the wicking behaviour of circular cross-section filament yarns. For instance, the experimental maximum wicking height for Sample 1 (0.07 mm) is 58 mm, whereas for Sample 4 (0.13 mm), it reduces to 35 mm. This observation is consistent with the general understanding that finer filaments tend to exhibit higher wicking capabilities due to their increased surface area and capillary action.

The observed correlation between filament diameter and wicking height enhances our comprehension of capillary behaviour in circular cross-section filament yarns. This newfound understanding carries significant implications for diverse applications, notably in textiles, optimal wicking performance influences moisture management. Additionally, the insights gained hold relevance in filtration processes, where capillary action plays a vital role in separating particles.

Moreover, the findings bear relevance in fluid transport systems employing filament yarns, providing a basis for enhancing efficiency and precision in various engineering applications.

Table 5.8. Maximum wicking height of C-shape cross-section filament yarns.

	Outer Diameter (mm)	**Inner Diameter (mm)**	**Experimental Maximum Wicking Height (mm)**	**Theoretical Maximum Wicking Hight Using D_{CH} (mm)**	**Theoretical Maximum Wicking Hight Using D_{CCH} (mm)**
Sample 5	0.07	0.03	77	52.19	80.70
Sample 6	0.09	0.03	65	44.72	69.17
Sample 7	0.11	0.04	57	36.05	60.52
Sample 8	0.13	0.05	45	31.75	48.42

In the investigation, we encountered an unexpected outcome as the D_{CH} approach, designed to consider pore geometry utilizing the C Shape profile, diverged from initial expectations by not aligning with the experimental results. Specifically, in the case of Sample 5, where the experimental maximum wicking height measured 77 mm, the D_{CH} approach yielded a prediction of 52.19 mm. Conversely, the alternative approach, the D_{CCH} method, which defines pore geometry by considering the cavity within the C-shaped profile as the pore, demonstrated a more favourable correspondence with the experimental findings. Particularly noteworthy is the case of Sample 5, where the theoretical maximum wicking height using D_{CCH} closely mirrored the experimental value, measuring 80.70 mm against the observed 77 mm.

In contrast to the established pattern of higher wicking for finer filaments observed in both mathematical and experimental assessments of circular filaments, the maximum wicking height in C-shaped filaments is notably contingent upon the diameter of the core within the structure, rather than the outer filament diameter.

5.3.9 Summary

In conclusion, our meticulous examination of experimental results reveals a remarkable agreement between calculated and observed maximum wicking heights for circular cross-section filament yarns. This robust correlation underscores the effectiveness of our theoretical model in capturing the intricate wicking behaviour inherent in circular filaments. The observed correlation between filament diameter and wicking height deepens our understanding of capillary behaviour in circular cross-section filament yarns, offering valuable insights with broad applications in textiles, filtration processes, and fluid transport systems. However, the unexpected divergence of the D_{CH} approach for C-shaped filaments prompted an alternative perspective using the D_{CCH} method, which exhibited a more favourable correspondence with experimental findings. This unexpected behaviour in C-

shaped filaments, notably dependent on the core diameter, deviates from established trends observed in circular filaments.

The research successfully integrates mathematical modelling and experimental validation to elucidate the wicking behaviour of C-shaped cross-section multifilament yarns. The precision of our theoretical models, validated by experimental results, provides valuable insights for optimizing filament yarn design and enhancing wicking performance across diverse applications.

5.4 Fabric Moisture Management Assessment through Advanced Image Analysis

In the field of textile engineering and moisture management, an accurate assessment of fabric-wicking properties is essential. This chapter presents a revolutionary instrument tailored for the precise determination of horizontal wicking in fabrics. Utilizing periodic imaging and MATLAB analysis, this innovative tool monitors moisture propagation across the fabric's surface. Research findings underscore the comparability between measurements obtained with our tester and conventional methods, highlighting its consistent and uniform results. The newly developed instrument, known for its affordability and practicality, addresses challenges related to cost and manual errors, making it a valuable asset for both extensive research endeavours and smaller industries within the textile sector.

5.4.1 Instrument Construction and Operation:

The Wicking Test Instrument is designed to assess fabric moisture management properties. It features a 100 cm2 flat sweating plane, a solenoid valve controlled by an Arduino Uno, and precise water dispensing for reproducible measurements. The instrument captures liquid spreading into the fabric over time, providing nuanced insights into moisture absorption.

Capturing Fabric Wicking: Fabric samples are placed on an illuminated 10x10 cm^2 table, and a solenoid valve dispenses a predetermined water drop, initiating the wicking process. A camera captures images at 10-second intervals and stored them to determine the wicking area.

Image Analysis: Digital Image Processing techniques in MATLAB software are employed for image analysis. The process involves capturing images with a 3.2-megapixel camera under controlled conditions for consistent results.

5.4.2 Experimental Methods and Materials

In Chapter 5.5.1, it's crucial to highlight the continuity in experimental materials and the manual calculation method for horizontal wicking, which aligns with the specifics outlined in Chapter 5.5.2. Wicking Evaluation through Image Analysis with the Developed Instrument

In the Horizontal Wicking by Image Analysis with the Developed Instrument segment, fabric wicking evaluation is enhanced. A 10x10 cm^2 fabric sample is placed on an illuminated table, and a precisely measured wicking solution is introduced through a solenoid valve. The wicking process is documented, and computer analysis of 5 images captures the absorbency rate, offering a visual understanding of moisture spread over one minute.

5.4.3 Results and Discussions

Five tests were conducted in both methods for the above sample to compute the average wicking area values. The wicking area measurements using the traditional AATCC 198-2011 manual method and our newly developed instrumental approach at various time intervals were noted immediately after 50 μL of water was allowed to fall on the fabric. The following table 5.9 presents the wicking area results in mm square for different fabric samples:

Table 5.9. Measured wicking area in mm square

Sample	AATCC 198-2011 Manual Method	Image Analysis with MATLAB					
	After 60 sec	After 10 sec	After 20 sec	After 30 sec	After 40 sec	After 50 sec	After 60 sec
Single Jersey	725	110	171	338	496	565	678
Lock Knit	1022	128	234	498	784	882	982
Matty	813	135	208	405	602	687	824.4
Crepe	823	148	228	448	659	749	898.8

5.4.4 Summary

This study introduces the Moisture Management Tester, a novel instrument for fabric moisture assessment through advanced image analysis. Using MATLAB, it5.9 aligns well with conventional methods, showing minor variations (11.4 mm^2 to 75.8 mm^2) for fabric samples (Single Jersey, Lock Knit, Matty, Crepe). The tool's efficiency, automation, and time-dependent analysis enhance fabric moisture assessments, making it valuable for research and production in the textile industry. Ongoing efforts include further analyses and testing scenarios for broader applicability in evaluating fabric comfort properties.

6 Conclusion

This study summarizes a comprehensive exploration into the optimization of thermal comfort properties in man-made fibrous textiles. The literature review unveils progressive developments in fibre structure, cross-section, and surface design, emphasizing strategies such as micro and nano fibres, along with the strategic blending of hydrophobic and hydrophilic materials, to enhance moisture transport and expedite drying in fabrics.

The scrutiny of physical and chemical finishing processes underscores the role of techniques like calendaring and plasma treatment in modifying fabric structure for improved moisture absorption and wicking. It is acknowledged, however, that these processes come with additional costs and potential reductions in physical performance. While chemical finishing methods, including cationization and the application of hydrophilic polymers, show promise in enhancing hydrophilicity and fabric comfort, their long-term efficacy requires further consideration.

The investigation into the wicking behaviour of polyester filament yarns, particularly those employed in sportswear, provides crucial insights into the impact of filament properties on wicking performance. The study identifies filament denier, cross-sectional shape, and intermingling processes as pivotal factors influencing wicking heights. Extending the research to knitted fabrics underscores the significance of fabric structure in water absorption, guiding fabric selection for sportswear applications.

The exploration of C-shaped cross-section filament yarns reveals their superior wicking performance compared to circular counterparts, positioning them as promising candidates for comfort fabrics in sportswear and activewear.

The thesis culminates with the introduction of the Moisture Management Tester, an innovative instrument for fabric moisture assessment utilizing advanced image analysis. This tool, alongside conventional methods, demonstrates efficiency, automation, and time-dependent analysis, enhancing its value for fabric moisture assessments in textile industry research and production. Ongoing efforts are directed toward further analyses and testing scenarios to broaden the tool's applicability in evaluating fabric comfort properties.

In essence, the findings contribute significantly to the ongoing discourse on achieving superior thermal comfort in man-made fibrous textiles, establishing them as versatile and comfortable alternatives in diverse applications.

7 Future Scope

This thesis studies polyester filament yarn wicking, considering denier, cross-section, and intermingling. It extends to knitted fabrics, highlighting their role in water absorption, especially in sportswear. Future research: refine filament properties, explore unconventional cross-sections, optimize fabric structures, and integrate advanced moisture assessment tools. Thorough field studies will enhance understanding of thermal comfort, fostering innovative advancements.

7.1 Future Directions for Enhanced Comfort in Man-Made Fibrous Textiles

1. In-depth Filament Property Analysis: Future research could broaden the scope by exploring a more extensive range of filament properties, including variations in molecular structure and surface treatments, to uncover additional factors influencing wicking behaviour.

2. Fabric Structure Optimization: Investigating additional knit structures and their impact on both vertical and horizontal wicking behaviours can offer valuable insights for fabric selection in diverse scenarios.

3. Exploration of Novel Filament Cross-sections: The promising outcomes from exploring C-shaped cross-section filament yarns suggest that unconventional filament shapes could significantly impact wicking performance. Future research could concentrate on the development and analysis of novel filament cross-sections for potential applications in comfort fabrics for sportswear and activewear.

4. Advanced Fibre Technologies: The ongoing evolution of fibre technologies, particularly in micro and nano fibres, presents an exciting avenue for further improving moisture management properties. Future research endeavours could focus on the development of novel fibres with enhanced capabilities for moisture transport and quick drying.

5. Refinement of Finishing Processes: The insights gained from exploring physical and chemical finishing processes highlight their potential, but there is a need for further research to refine these techniques. Future studies might delve into assessing the long-term effects of these finishes on fabric comfort properties, ensuring their reliability and durability over extended usage.

In summary, the future scope of research in this domain involves continuous exploration and innovation in fibre technologies, blending strategies, finishing processes, filament properties, fabric structures, and moisture assessment tools.

8 Publications

Sr. No.	Publications/Presentation Details
1	Title: Developments in profile filament yarn for enhancing moisture management properties of fabrics. Name of Journal: Man-Made Textiles in India. (Scopus link- Type of Journal: Scopus Status: Published on March 2020, 48 (3): 88-92. Authors : Sujit Gulhane & Dr. P. P. Raichurkar
2	Title: Wicking Properties of Knitted Sportswear Fabrics Composed of Polyester Filament Yarns Name of Journal: Colourage Type of Journal: Scopus Status: Published on May 2021, Issue 68- vol 5 pages 27-32. Authors: Sujit Gulhane & Dr. Vijay Shivankar
3	Title: Wicking Performance of C-Shape Filament Yarn for Comfort Fabrics Name of Journal: Journal of Textile Association, Type of Journal: Scopus Status: Submitted on 28th Aug, Accepted on 28th Sep. 2023 for Nov-Dec 2023 Issue. Authors: Sujit Gulhane & Dr. Vijay Shivankar
4	Title: Finishing Techniques for Enhancing Moisture Management in Synthetic Fabrics Name of Journal: Man-Made Textile in India Type of Journal: Scopus Status: Submitted on 5th Dec.2023. Authors: Sujit Gulhane & Dr. Vijay Shivankar
5	Title: Development of Mathematical Model for C Shape Filament Yarn Wicking Name of Journal: Indian Journal of Fibre & Textile Research Type of Journal: SCI, Scopus Status: Submitted on 26th Dec 2023. Authors: Sujit Gulhane & Dr. Vijay Shivankar
6	Title: Wicking Behaviour of Polyester Filament Yarns Used in Sportswear Name of Conference: 'International Conference on Advances in Technical Textiles (ICATT-2020)', Bannari Amman Institute of Technology Type of Conference: International Status: Presented on 24th Oct 2020. Authors: Sujit Gulhane & Dr. Vijay Shivankar
7	Title: A Wicking Behaviour of Profile Filament Yarn Knitted Fabrics. Name of Conference: National Conference on Futuristic Trends in Textiles, CTF, NMIMS, Shirpur Type of Conference: National

	Status: Presented on 20th February 2021. Authors: Sujit Gulhane & Dr. Vijay Shivankar
8	Title: Enhancing Fabric Moisture Management Assessment through Advanced Image Analysis Name of Conference: Digital Technology Vision 2030: Transforming Healthcare, Education, and Industry. Type of Conference: International Status: Extended Abstract Accepted on 23rd Dec.2024. Authors: Sujit Gulhane & Dr. Vijay Shivankar
9	Indian Patent Title: Fabric Horizontal Wicking Tester Using Image Analysis. Application No. 202021034709 Status: Published in Indian Patent Journal 05 Aug. 2022 Authors: Sujit Gulhane & Dr. Vijay Shivankar

9 References

[1] A. Rajan, A. Singh, and P. Chaudhary, "MANMADE FIBRE INDUSTRY OUTLOOK 2022," *Textile Value Chain*, Sep. 26, 2022.

[2] V. G. Gorade, B. U. Chaudhary, and R. D. Kale, "Polyester fabric with moisture management properties using a sol–gel technique for activewear," *Journal of Polymer Research*, vol. 28, no. 8, 2021, doi: 10.1007/s10965-021-02650-7.

[3] Y. Jhanji, D. Gupta, and V. K. Kothari, "Thermo-physiological properties of polyester–cotton plated fabrics about fibre linear density and yarn type," *Fashion and Textiles*, vol. 2, no. 1, 2015, doi: 10.1186/s40691-015-0041-x.

[4] S. S. Gulhane and P. P. Raichurkar, "Developments in profile filament yarn for enhancing moisture management properties of fabrics," *Man-Made Textiles in India*, vol. 48, no. 3, 2020.

[5] M. Senthilkumar, M. B. Sampath, and T. Ramachandran, "Moisture Management in an Active Sportswear: Techniques and Evaluation—A Review Article," *Journal of The Institution of Engineers (India): Series E*, vol. 93, no. 2, 2012, doi: 10.1007/s40034-013-0013-x.

[6] A. Patnaik, R. S. Rengasamy, V. K. Kothari, and A. Ghosh, "Wetting and wicking in fibrous materials," *Textile Progress*, vol. 38, no. 1, 2006, doi: 10.1533/jotp.2006.38.1.1.

[7] S. Sonawane, P. W. Chandurkar, P. P. Kolte, and P. P. Raichurkar, “Role of developed card technology in the improvement of yarn quality,” *Melliand International*, vol. 24, no. 3, 2018.

[8] M. B. Sampath and M. Senthilkumar, “Effect of Moisture management finish on comfort characteristics of microdenier polyester knitted fabrics,” *Journal of Industrial Textiles*, vol. 39, no. 2, 2009, doi: 10.1177/1528083709102922.

[9] M. Sarkar, J. Fan, and X. Qian, “Transplanar water transport tester for fabrics,” *Meas Sci Technol*, vol. 18, no. 5, 2007, doi: 10.1088/0957-0233/18/5/036.

[10] D. Raja, G. Ramakrishnan, V. R. Babu, M. Senthilkumar, and M. B. Sampath, “Comparison of different methods to measure the transverse wicking behaviour of fabrics,” *Journal of Industrial Textiles*, vol. 43, no. 3, 2014, doi: 10.1177/1528083712456054.

[11] A. P. D’Silva, C. Greenwood, S. C. Anand, D. H. Holmes, and N. Whatmough, “Concurrent determination of absorption and wickability of fabrics: A new test method,” *Journal of the Textile Institute*, vol. 91, no. 3, 2000, doi: 10.1080/00405000008659515.

[12] R. M. Laing, B. E. Niven, R. L. Barker, and J. Porter, “Response of Wool Knit Apparel Fabrics to Water Vapor and Water,” *Textile Research Journal*, vol. 77, no. 3, 2007, doi: 10.1177/0040517506069157.

[13] “AATCC TM195, Liquid Moisture Management Properties of Textile Fabrics,” *American Association of Textile Chemists and Colorists*. 2009.

[14] J. hu, yi li, K. W. Yeung, A. S. W. Wong, and W. xu, “Moisture Management Tester: A Method to Characterize Fabric Liquid Moisture Management Properties,” *Textile Research Journal*, vol. 75, no. 1, 2005, doi: 10.1177/004051750507500111.

[15] M. M. Adler and W. K. Walsh, “Mechanisms of Transient Moisture Transport Between Fabrics,” *Textile Research Journal*, vol. 54, no. 5, 1984, doi: 10.1177/004051758405400510.

[16] M. Manshahia and A. Das, “Thermophysiological comfort characteristics of plated knitted fabrics,” *Journal of the Textile Institute*, vol. 105, no. 5, 2014, doi: 10.1080/00405000.2013.826419.

[17] R. Fangueiro, A. Filgueiras, F. Soutinho, and X. Meidi, “Wicking Behaviour and Drying Capability of Functional Knitted Fabrics,” *Textile Research Journal*, vol. 80, no. 15, 2010, doi: 10.1177/0040517510361796.

[18] C. I. su, J. X. Fang, X. H. Chen, and W. Y. wu, "Moisture Absorption and Release of Profiled Polyester and Cotton Composite Knitted Fabrics," *Textile Research Journal*, vol. 77, no. 10, 2007, doi: 10.1177/0040517507080696.

[19] T. Hussain, A. Nazir, and R. Masood, "Liquid Moisture Management in Knitted Textiles – A Review," *3rd International Conference on Value Addition & Innovation in Textiles (Covitex-2015)*, no. MARCH, 2015.

[20] M. B. Sampath, S. Mani, and G. Nalankilli, "Effect of filament fineness on comfort characteristics of moisture management finished polyester knitted fabrics," *Journal of Industrial Textiles*, vol. 41, no. 2, 2011, doi: 10.1177/1528083711400774.

[21] M. Abu-Rous, E. Ingolic, and K. C. Schuster, "Visualisation of the Nano-Structure of Tencel®(Lyocell) and Other Cellulosics as an Approach to Explaining Functional and Wellness Properties in Textiles," *Lenzinger Berichte*, vol. 85, 2006.

[22] P. Sakthi, K. Sangeetha, and M. Bhuvaneshwari, "Development of double layer knitted fabric for sportswear using tencel/polypropylene fibres," *International Journal of Current Research and Review (IJCRR)*, vol. 8, no. 6, 2016.

[23] D. Raja, C. Prakash, G. Ramakrishnan, and C. V. Koushik, "Influence of blend ratio and linear density on liquid spreading characteristics of bamboo/cotton-blended yarn knitted fabrics measured by liquid spread tester," *Journal of the Textile Institute*, vol. 105, no. 8, 2014, doi: 10.1080/00405000.2013.856075.

[24] C. Prakash, G. Ramakrishnan, and C. V. Koushik, "Effect of blend proportion on moisture management characteristics of bamboo/cotton knitted fabrics," *Journal of the Textile Institute*, vol. 104, no. 12, 2013, doi: 10.1080/00405000.2013.800378.

[25] O. Troynikov and W. Wardiningsih, "Moisture management properties of wool/ polyester and wool/bamboo knitted fabrics for the sportswear base layer," *Textile Research Journal*, vol. 81, no. 6, 2011, doi: 10.1177/0040517510392461.

[26] M. Manshahia and A. Das, "Moisture management of high active sportswear," *Fibres and Polymers*, vol. 15, no. 6, 2014, doi: 10.1007/s12221-014-1221-9.

[27] F. Wang, X. Zhou, and S. Wang, "Development processes and property measurements of moisture absorption and quick dry fabrics," *Fibres and Textiles in Eastern Europe*, vol. 73, no. 2, 2009.

[28] O. Demiryürek and D. Uysaltürk, “Thermal comfort properties of Viloft/cotton and Viloft/polyester blended knitted fabrics,” *Textile Research Journal*, vol. 83, no. 16, 2013, doi: 10.1177/0040517513478458.

[29] “Toray Introducing Airfine Fieldsensor’,” *JTN Weekly*, vol. 24, no. 35, 1998.

[30] M. Blaga, A. Marmarali, and A. Mihai, “Functional knitted fabrics for footwear linings,” *Tekstil ve Konfeksiyon*, vol. 21, no. 1, 2011.

[31] R. Guruprasad, M. V. Vivekanandan, A. Arputharaj, S. Saxena, and S. K. Chattopadhyay, “Development of cotton-rich/polylactic acid fibre blend knitted fabrics for sports textiles,” *Journal of Industrial Textiles*, vol. 45, no. 3, 2015, doi: 10.1177/1528083714555779.

[32] K. T. Yilma and D. Y. Limeneh, “Review on Moisture Management Finish: Mechanism and Evaluation,” *Journal of Natural Fibres*, vol. 19, no. 14. 2022. doi: 10.1080/15440478.2021.1966566.

[33] R. N. P. Gunarathna, T. Sandanuwan, D. A. S. Amarasinghe, D. Attygalle, S. C. Weragoda, and N. Hendeniya, “Moisture transportation in polyester fabrics by plasma printed wicking channels,” in *MERCon 2021 - 7th International Multidisciplinary Moratuwa Engineering Research Conference, Proceedings*, 2021. doi: 10.1109/MERCon52712.2021.9525725.

[34] M. Akgun, M. Kanik, S. Seçmen, M. Macit, and E. Gülşen, “Research on the Method for Controlling the Liquid Absorptivity Behaviour of Polyester Textile Materials,” *AATCC Journal of Research*, vol. 9, no. 3, 2022, doi: 10.1177/24723444221084395.

[35] M. Zaman, H. Liu, H. Xiao, F. Chibante, and Y. Ni, “Hydrophilic modification of polyester fabric by applying nanocrystalline cellulose containing surface finish,” *Carbohydr Polym*, vol. 91, no. 2, 2013, doi: 10.1016/j.carbpol.2012.08.070.

[36] A. B. Nyoni and D. Brook, “Wicking mechanisms in yarns-the key to fabric wicking performance,” *Journal of the Textile Institute*, vol. 97, no. 2, 2006, doi: 10.1533/joti.2005.0128.

[37] A. Perwuelz, M. Casetta, and C. Caze, “Liquid organisation during capillary rise in yarns - influence of yarn torsion,” *Polym Test*, vol. 20, no. 5, 2001, doi: 10.1016/S0142-9418(00)00075-1.

[38] B. Das, A. Das, V. K. Kothari, and R. Fangueiro, “Development of mathematical model to predict vertical wicking behaviour.part I: flow through yarn,” *Journal of the Textile Institute*, vol. 102, no. 11, 2011, doi: 10.1080/00405000.2010.529281.

[39] Y. K. Kamath, S. B. Hornby, H. D. Weigmann, and M. F. Wilde, “Wicking of Spin Finishes and Related Liquids into Continuous Filament Yarns,” *Textile Research Journal*, vol. 64, no. 1, 1994, doi: 10.1177/004051759406400104.

[40] A. Perwuelz, P. Mondon, and C. Caze, “Experimental Study of Capillary Flow in Yarns,” *Textile Research Journal*, vol. 70, no. 4, 2000, doi: 10.1177/004051750007000409.

[41] Q. Zhuang, S. C. Harlock, and D. B. Brook, “Longitudinal wicking of weft knitted fabrics part II: Wicking mechanism of knitted fabrics used in undergarments for outdoor activities,” *Journal of the Textile Institute*, vol. 93, no. 1, 2002, doi: 10.1080/00405000208630555.

[42] C. Prahsarn, R. L. Barker, and B. S. Gupta, “Moisture Vapor Transport Behaviour of Polyester Knit Fabrics,” *Textile Research Journal*, vol. 75, no. 4, 2005, doi: 10.1177/0040517505053811.

[43] “AATCC TM197-2022, Vertical Wicking Rate of Textiles: to Specified Distances,” *American Association of Textile Chemists and Colorists*, 2011.

[44] “AATCC TM198,, Horizontal Wicking of Textiles,” *American Association of Textile Chemists and Colorists*. 2011.

[45] F. W. Minor, A. M. Schwartz, E. A. Wulkow, and L. C. Buckles, “The Migration of Liquids in Textile Assemblies,” *Textile Research Journal*, vol. 29, no. 12, 1959, doi: 10.1177/004051755902901201.

[46] W. Zhong, X. Ding, and Z. L. Tang, “Modeling and Analyzing Liquid Wetting in Fibrous Assemblies,” *Textile Research Journal*, vol. 71, no. 9, 2001, doi: 10.1177/004051750107100903.

[47] E. Kissa, “Wetting and Wicking,” *Textile Research Journal*, vol. 66, no. 10, 1996, doi: 10.1177/004051759606601008.

[48] E. W. Washburn, “The dynamics of capillary flow,” *Physical Review*, vol. 17, no. 3, 1921, doi: 10.1103/PhysRev.17.273.

[49] X. Chen, K. G. Kornev, Y. K. Kamath, and A. V. Neimark, “The Wicking Kinetics of Liquid Droplets into Yarns,” *Textile Research Journal*, vol. 71, no. 10, 2001, doi: 10.1177/004051750107101003.